

# Three concentric rings as frequency selective surfaces on isotropic chiral slabs

S. UÇKUN\*, T. EGE

*Department of Electrical and Electronics Engineering, University of Gaziantep, 27310, Gaziantep, Turkey*

Frequency-selective surfaces (FSSs) have attracted the attention of many researchers and different methods have been developed to analyze different types of FSS structures. One of the typical FSSs is rings printed on a dielectric substrate. In this study, the arrays of three-concentric conducting rings printed on an isotropic chiral slab are investigated and transmission/reflection characteristics are presented. The analysis used is based on the Modal Analysis and Method of Moments combined with the Floquet Theorem.

(Received August 29, 2005; accepted January 26, 2006)

*Keywords:* Frequency selective surface, Chiral, Three-concentric rings

## 1. Introduction

Frequency Selective Surfaces (FSSs), which are periodic structures that provide different characteristics over different frequency bands, have been the subject of extensive study over the last decades [1-2] and they find wide applications in satellite communication systems and filters in microwaves and optics. Typically, an FSS consists of periodically arranged metallic patch elements on a dielectric substrate or aperture elements within a metallic screen. Such structure shows total reflection or transmission in the resonance region. Some of the factors that affect the performance and behavior of a single screen FSS can be counted as the geometry of the FSS element, permittivity of the FSS slab, period of the FSS array, conductivity of the FSS conductor, angle of incidence and polarization of the incoming wave. Typical applications of FSSs include dual-band [2] and triple-band [3] antennas, reflector antennas [4], radoms [5], absorbers [6] and polarizers [7].

Chiral media have also received considerable attention in recent years due to its potential applications in the fields of electromagnetics and microwaves. A linearly polarized wave incident on a chiral slab splits into two circularly polarized waves, left and right, with phase velocities different from each other. The two circularly polarized waves combine and a linearly polarized wave, whose plane of polarization is rotated with respect to plane of polarization of the incident plane wave, emerge behind the chiral slab. The amount of the rotation or attenuation depends on the distance traveled in the medium and on the difference between the two wave numbers, which is an indication of the degree of chirality given by  $\xi$ . The propagation of electromagnetic waves through an infinite slab of chiral medium is formulated in [8] for oblique incidence and solved analytically for the case of normal incidence. Different applications of isotropic chiral materials in microwave and antenna engineering can be found in literature, as in chiro-waveguides, microstrip structures, periodic achiral-

chiral interfaces, anti-reflection coatings and FSSs [9-10]. Experimental investigations on arrays of elements of different shapes like Jerusalem cross, circular ring, the square loop have been carried out earlier [11-12]. Despite the many years of FSS research, new designs still appear and no doubt will continue to do so. During recent years we have witnessed the examination of dielectric slabs in FSSs through their replacement by isotropic chiral [13-14], anisotropic [15-16] and uniaxial chiral slabs [17]. Circular geometries have also proved to be useful FSS elements [18]. They can be used as dual polarized FSS elements. A model analysis of a single screen FSS with two ring patch element was presented by Parker et al. [19] on a dielectric substrate. The analysis of single circular rings on isotropic chiral slabs is given by [13]. Two-concentric rings on isotropic chiral slabs has been sent by the authors of this paper to a journal for consideration for publication but to the best of our knowledge, there is no study of three-concentric rings on isotropic chiral slabs.

This paper presents the results obtained in a theoretical investigation of the scattering by an FSS consisting of an infinite array of three-concentric rings arranged in a doubly periodic grid on a chiral slab, as shown in Fig. 1. The motivation behind this work is that the three-concentric rings is an original approach to the conception of multiple resonant frequency bands. In addition to this, introduction of chirality to the backing dielectric slab in three-concentric rings structure offers an extra design parameter which can be exploited to improve the spectral characteristics of the FSS. The numerical results of transmission characteristics of an isotropic chiral slab with three-concentric rings on it are presented. A full-wave analysis for the problem of scattering by Chiro-FSS is presented by Koca and Ege in detail [14]. The analysis is based on the Modal Analysis and Method of Moments combined with the Floquet Theorem. In their paper, numerical results of reflection and transmission characteristics of Chiro-FSSs with cross dipoles, circular rings and rectangular plates are presented for normal incidence.

## 2. Theory

An isotropic, homogeneous, lossless and source free chiral medium can be described electromagnetically (assuming  $e^{j\omega t}$  time dependence) by the constitutive relations,

$$\mathbf{D} = \epsilon \mathbf{E} - j\xi \mathbf{B} \quad (1a)$$

$$\mathbf{H} = -j\xi \mathbf{E} + (1/\mu_c) \mathbf{B} \quad (1b)$$

where  $\xi$  is the chirality admittance, and  $\epsilon_c$  and  $\mu_c$  are the permittivity and permeability of the isotropic chiral medium, respectively. In this study all the constitutive parameters are assumed to be real quantities, as in [21-23]. Using equations (1a) and (1b) together with the time harmonic Maxwell's equations for a source free isotropic chiral medium one can obtain the chiral Helmholtz equation as

$$\nabla \times \nabla \times \mathbf{E} - 2\omega\mu_c \xi \nabla \times \mathbf{E} - \omega^2 \mu_c \epsilon_c \mathbf{E} = 0 \quad (2a)$$

$$\nabla \times \nabla \times \mathbf{H} - 2\omega\mu_c \xi \nabla \times \mathbf{H} - \omega^2 \mu_c \epsilon_c \mathbf{H} = 0 \quad (2b)$$

From these equations it is found that propagating eigenmodes within such media consists of two circularly polarized waves with characteristic wave numbers,

$$k_R = \omega\mu_c \xi + \sqrt{k^2 + (\omega\mu_c \xi)^2} \quad (3a)$$

$$k_L = -\omega\mu_c \xi + \sqrt{k^2 + (\omega\mu_c \xi)^2} \quad (3b)$$

where  $k_R$  and  $k_L$  are real quantities for propagating waves. Hence the chiral medium allows double mode propagation as left hand circularly polarized (LCP) and right hand circularly polarized (RCP) waves with different phase velocities of  $v_L = \omega/k_L$  and  $v_R = \omega/k_R$ , respectively. The relation between the electric and magnetic fields can be written as,

$$\mathbf{E} = \frac{1}{j\omega(\epsilon_c + \mu_c \xi^2)} (\nabla \times \mathbf{H} - \omega\mu_c \xi \mathbf{H}) \quad (4)$$

$$\mathbf{H} = -\frac{1}{j\omega\mu_c} (\nabla \times \mathbf{E} - \omega\mu_c \xi \mathbf{E}) \quad (5)$$

Three concentric rings are placed periodically on the x-y plane, as shown in Fig. 1. It is assumed to be infinitely thin and a perfect conductor. Due to the periodicity of the problem the fields are expanded into Floquet modes in the air and chiral regions. The amplitude coefficients of the right and left circularly polarized scattered waves traveling in the forward and backward directions in the three regions can be expressed in terms of the induced current density  $\mathbf{J}(x,y)$  on the conducting element of a single unit cell by using the following boundary conditions;

- i. tangential electric and magnetic fields are continuous at  $z = d$ .
- ii. tangential electric field is continuous at  $z = 0$ .

- iii. tangential magnetic field is discontinuous at  $z = 0$  by an amount equal to  $\mathbf{J}(x,y)$ .

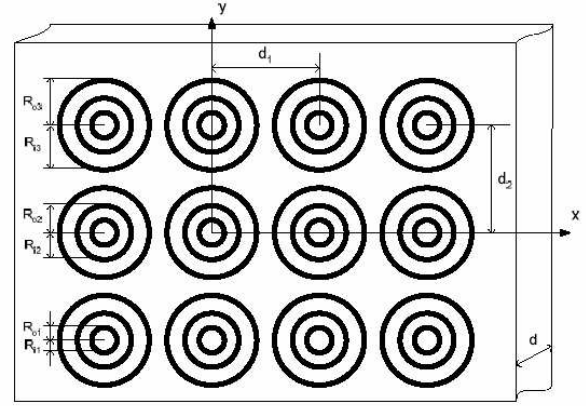


Fig. 1. Geometry of three dimensional arrays of thin conducting three-concentric rings.

These boundary conditions combined with the Floquet modes orthogonality condition over a single periodic unit cell lead to a Fredholm integral equation of the first kind for the unknown current density induced on the metallic part of the three concentric rings by the incident plane wave. This integral equation can be solved using the moments method as follows: To obtain a formulation of the problem suitable for numerical computations it is necessary to reduce the integral equation to a matrix equation which may be solved by matrix inversion. For this, as used in [14], the unknown current density on the rings along the circumference is first expressed as a finite sum of orthogonal sine and cosine functions with undetermined coefficients:

$$\mathbf{J}(\varphi) = \sum_{r=1}^3 \left[ \sum_{n=0}^N a_n \cos n\varphi + \sum_{n=1}^M b_n \sin n\varphi \right] \mathbf{a}_\varphi \quad (6)$$

where  $\varphi$  is the angular position of a point on the circumference of a ring centered at the origin.

The integral equation is then transformed into matrix equation by enforcing the boundary condition where the total electric field is zero on the rings using Galerkin's testing procedure. A complex matrix inversion program is implemented to obtain the solutions of the resulting matrix equation. The transmission and reflection coefficients can be computed in a straightforward manner.

## 3. Numerical results

In this section, the curves of the transmission/reflection coefficients versus frequency are shown for the FSSs on isotropic chiral layers. To verify the accuracy of the computed results, the characteristics given for free-standing FSSs in literature are compared with the results obtained from our program running with zero chiral admittance [18-20]. As expected, the agreement between these results and the values given in literature is very good both for single ring and two-

concentric rings. Convergence of the numerical results has been studied by varying the number of current terms and Floquet harmonics. For all figures we assumed that the magnetic vector is parallel to the plane of the FSS (TM incidence). Consider an infinite array of free-standing circular rings which are arranged in a square lattice with  $d_1=d_2=10$  mm. The inner and outer radii of the single ring are  $R_{i1} = 2.65$  mm and  $R_{o2} = 3.35$  mm, respectively. Fig. 2 shows the variation of the TM transmission coefficient with frequency. As seen, there exists one resonant frequency for the free-standing single ring and this frequency,  $f_R$ , is approximately equal to  $c / [2\pi (R_i + 0.5w)]$ , where  $R_i$  is its inner radius and  $w$  is its width [11]. When the number is increased to two-concentric rings, similar to the geometry of Fig. 1, our expectation will be two resonant frequencies at two different points, as seen in Fig. 2. Again the elements are centered on a square lattice of side  $d_1 = d_2 = 10$  mm. The inner and outer radii of the inner ring are  $R_{i1} = 2.65$  mm and  $R_{o1} = 3.35$  mm, respectively. Similarly, the inner and outer radii of the outer ring are  $R_{i2} = 3.7$  mm and  $R_{o2} = 4.7$  mm, respectively. When the number of rings is increased to three, with the geometry of Fig. 1, one will expect three resonant frequencies at three different points, as seen again in Fig. 2. Again the elements are centered on a square lattice of side  $d_1 = d_2 = 10$  mm. The inner and outer radii of the two inner rings are the same as above two-concentric rings. Similarly, the inner and outer radii of the outer ring are  $R_{i3} = 5.7$  mm and  $R_{o3} = 6.7$  mm, respectively.

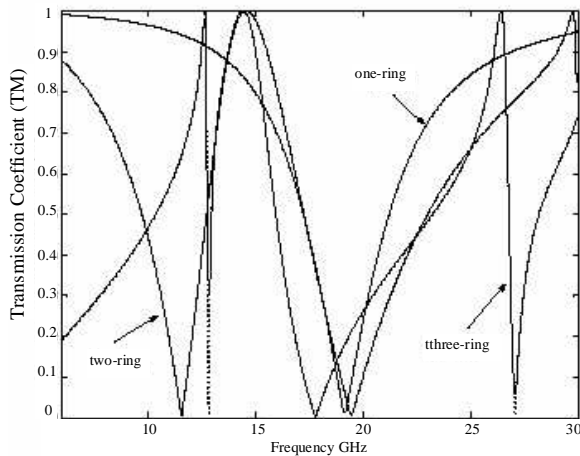


Fig. 2. TM transmission coefficient for one-, two- and three-concentric free-standing rings. ( $R_{i1} = 0.265$  cm,  $R_{o1} = 0.335$  cm,  $R_{i2} = 0.37$  cm,  $R_{o2} = 0.47$  cm,  $R_{i3} = 0.57$  cm,  $R_{o3} = 0.67$  cm,  $d_1 = d_2 = 1.0$  cm,  $\theta=0^\circ$ , lattice angle= $90^\circ$ ).

Next, these three-concentric ring arrays of square lattice geometry are considered on a 0.2 cm thick dielectric substrate with relative permittivity  $\epsilon_r = 1.06$ . The authors

of this study wish to observe the behaviors of three-concentric rings located on a chiral slab. Fig. 3 illustrates the transmission coefficient variances of three concentric-rings for free-standing and chiral slabs of two different chirality admittances. As will be seen from the same figure, increasing the chirality admittance shifts lower resonant frequency to the left. The middle resonant frequency is stable up to 0.0025 mho chirality admittance but we have third resonance around 23 GHz only for the highest chirality admittance for the given range of frequency.

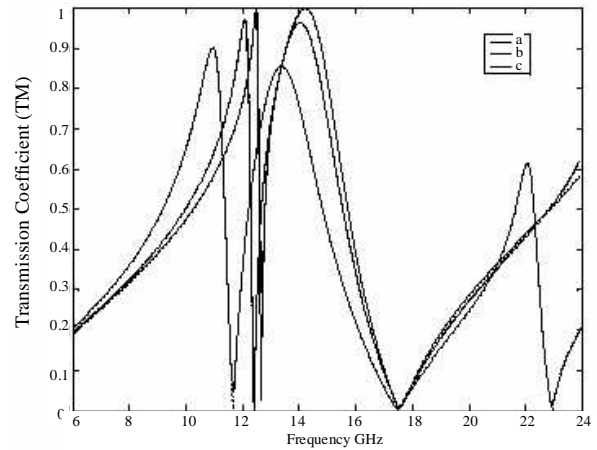


Fig. 3. TM transmission coefficient for Chiro-FSS with three-concentric rings ( $d=0.2$ ,  $\epsilon_r=1.06$ ,  $R_{i1}=0.265$  cm,  $R_{o1}=0.335$  cm,  $R_{i2}=0.37$  cm,  $R_{o2}=0.47$  cm,  $R_{i3} = 0.57$  cm,  $R_{o3} = 0.67$  cm,  $d_1 = d_2 = 1.0$  cm,  $\theta=0^\circ$ , lattice angle= $90^\circ$ ) a: Free-standing b:  $\zeta = 0.0012$  mho c:  $\zeta = 0.0025$  mho.

Figs. 4 and 5 give a comparison of the calculated reflection and transmission coefficients for a two dimensional periodic array of three-concentric rings on a 2 mm thick dielectric ( $\epsilon_r=1$  and  $\xi=0$ ), chiral slab with (0.0012 mho) and chiral slab with (0.0025 mho), which match the values used for Fig. 3. These results are obtained for the same array of three-concentric conducting rings as given in Fig. 3, but this time arranged in a triangular spacing with lattice angle  $60^\circ$  when the array is illuminated by a normally incident TM (co-polar) plane wave. As can be seen from Figs. 4 and 5, the reflected wave from Chiro-FSS has only co-polar component whereas due to the introduction of chiral material the transmitted wave has both co-polar (TM) and cross-polar (TE) components even at normal incidence. As seen in both figures, as the chirality admittance is increased, resonance frequency shifts to the lower frequencies. In Fig. 5, polarization conversion can also be observed for the transmitted fields from the Chiro-FSS. TM wave incident on a Chiro-FSS is converted into either TM or TE wave with total transmission in air on the other side.

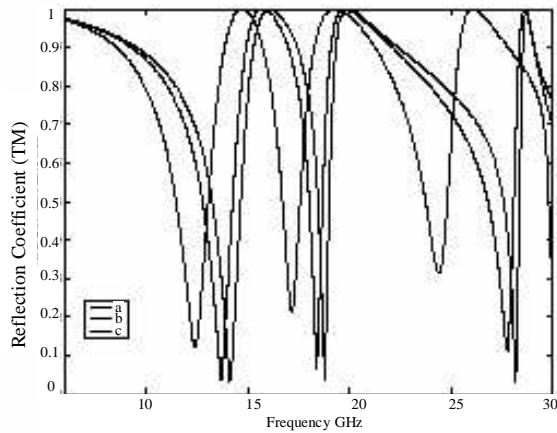


Fig. 4. TM reflection coefficient for Chiro-FSS with three-concentric rings. ( $d=0.2$ ,  $\epsilon_r=1.06$ ,  $Ri1=0.265\text{cm}$ ,  $Ro1=0.335\text{cm}$ ,  $Ri2=0.37\text{cm}$ ,  $Ro2=0.47\text{cm}$ ,  $Ri3=0.57\text{cm}$ ,  $Ro3=0.67\text{cm}$ ,  $d1=d2=1.0\text{cm}$ ,  $\theta=0^\circ$ , lattice angle  $=60^\circ$ ) a: Free-standing b:  $\xi=0.0012\text{mho}$  c:  $\xi=0.0025\text{mho}$ .

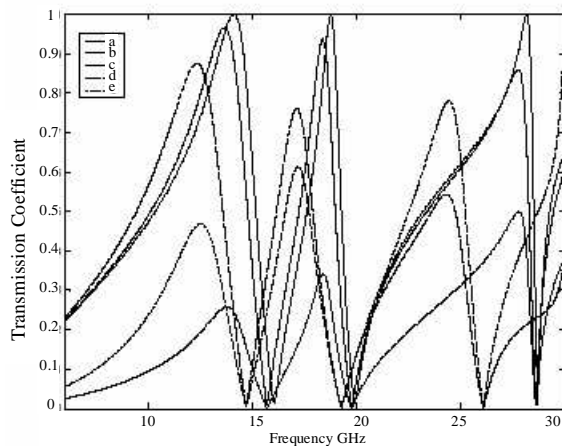


Fig. 5. TM transmission coefficient for Chiro-FSS with three-concentric rings. ( $d=0.2$ ,  $\epsilon_r=1.06$ ,  $Ri1=0.265\text{cm}$ ,  $Ro1=0.335\text{cm}$ ,  $Ri2=0.37\text{cm}$ ,  $Ro2=0.47\text{cm}$ ,  $Ri3=0.57\text{cm}$ ,  $Ro3=0.67\text{cm}$ ,  $d1=d2=1.0\text{cm}$ ,  $\theta=0^\circ$ , lattice angle  $=60^\circ$ ) a: Free-standing b: co-polar ( $\xi=0.0012\text{mho}$ ) c: cross-polar ( $\xi=0.0012\text{mho}$ ) d: co-polar ( $\xi=0.0025\text{mho}$ ) e: cross-polar ( $\xi=0.0025\text{mho}$ ).

#### 4. Conclusion

The transmission coefficients of the arrays of three-concentric conducting rings printed on an isotropic chiral slab are presented for different chirality parameters. As expected, three-concentric rings on a dielectric substrate produced three resonant frequencies. Replacing dielectric substrate with a proper isotropic chiral slab shifted resonant frequencies to the left, which indicates a strong possibility of increase in the number of resonant frequencies in a certain range of frequency.

The dielectric or chiral slab support affects the transmission response by lowering the resonant frequency and altering the bandwidths. It is observed that the

transmission coefficients of FSS with chiral slab are very much similar to those of the FSS with dielectric slab if the chirality admittance is small. Results indicate that Chiro-FSS provides a full reflection over multiple resonant frequency bands. Furthermore, the bandwidths associated with these multiple resonances are observed to be narrower than that of a free-standing FSS. Another important outcome of the study is that polarization conversion is possible for the transmitted fields from the Chiro-FSS. In other words, TM wave incident on a Chiro-FSS can be converted into either TM or TE wave with total transmission in air on the other side.

#### References

- [1] B. A. Munk, Periodic surface for large scan angles, US Patent **3**, 789, 404 (1974).
- [2] R. Mittra, C. C. Chan, T. Cwik, Techniques for analyzing frequency selective surfaces: a review, Proc IEEE **76**, 1593 (1988).
- [3] J. Huang, T. K. Wu, S. W. Lee, Tri-Band Frequency Selective Surface with Circular Ring Elements, IEEE Trans Antenna Propagat. **42**, 166 (1994).
- [4] N. D. Agrawal, W. A. Imbraile, Design of a dielectric cassegrain subreflector, IEEE Trans Antenna Propagat., **AP-27**, 466 (1979).
- [5] S. W. Lee, Scattering by dielectric loaded screen. IEEE Trans Antenna Propagat. **19**, 656 (1971).
- [6] C. Mias, Varactor tunable frequency selective absorber, Electron Lett **39**, 1060 (2003).
- [7] S. Uçkun, T. Ege, Computation of susceptance for thick meander-line polarizer, Electron Lett, **27**, 276 (1991).
- [8] S. Bassiri, C. H. Papas, N. Engheta, Electromagnetic Wave Propagation Through a Dielectric-Chiral Interface and Through a Chiral Slab, J. Opt. Soc. Am A **5**, 1450 (1988).
- [9] A. Lakhtakia, V. K. Varadan, V. V. Varadan, Time Harmonic Electromagnetic Fields in Chiral Media, Berlin: Springer-Verlag, 1989.
- [10] F. Bilotti, A. Toscano, L. Vegni, Analysis of Cavity-Backed Antennas with Chiral Substrates and Superstrates Using the Finite Element Method, Electromagnetics **24**, 3-12 (2004).
- [11] B. A. Munk, Frequency Selective Surfaces, Theory and Design, John Wiley&Sons Inc, 2000.
- [12] J. C. Vardaxoglou, Frequency Selective Surfaces, Analysis and Design, RSP, John Wiley&Sons Inc, 1997.
- [13] A. O. Koca, T. Ege, A Novel Frequency Selective Surface, Chiro-FSS, Microwave Opt. Technol. Lett. **10**, 157 (1995).
- [14] A. O. Koca, T. Ege, Frequency Selective Surfaces on Isotropic Chiral Slabs, AEÜ **52**, 17 (1998)
- [15] A. L. P. S. Campos, A. G. d'Assunção, A. Gomes Neto, Scattering Characteristics of FSS on two Anisotropic Layers for Incident Co-polarized Plane Waves, Microwave Opt. Technol. Lett. **33**, 57 (2002).

- [16] M. L. C. Gomes Neto, A. L. P. S. Campos, A. G. d'Assunção, Scattering Analysis of Frequency Selective Surfaces on Anisotropic Substrates Using the Hertz Vector-Potential Method, *Microwave Opt. Technol. Lett.* **44**, 67 (2005).
- [17] M. Asai, J. Yamakita, H. Wakabayashi, Analysis of Diffraction from Uniaxial Chiral Slab with a Two-Dimensional Array of Patches, *Electrical Engineering in Japan*, **147**, 1-8 (2004).
- [18] E. A. Parker, S. M. A. Hamdy, Rings as Elements for Frequency Selective Surfaces, *Electron Lett.* **17**, 612 (1981).
- [19] E. A. Parker, S. M. A. Hamdy, R. J. Langley, Arrays of Concentric Rings as Frequency Selective Surfaces, *Electron Lett.* **17**, 880 (1981).
- [20] P. Bielli, D. Bresciani et al., Study of dichroic subreflector for multi-frequency antennas, ESA Report, Contract 5355/83/NL/GM, 1984.
- [21] D. M. Pozar, Microstrip antennas and arrays on chiral substrates, *IEEE Trans Antennas, Propagat.* **AP-40**, 1260 (1992).
- [22] A. Lakhtakia, V. K. Varadan, V. V. Varadan, Scattering by Periodic achiral-chiral interface, *J. Opt. Soc. Am. A* **11**, 1675 (1989).
- [23] A. Lakhtakia, V. V. Varadan, V. K. Varadan, A parametric study of microwave reflection characteristics of a planar achiral-chiral interface, *IEEE Trans Electromag Compt EMC*, **28**, 90 (1986).

---

\* Corresponding author: savas@gantep.edu.tr